J|A|C|S
ARTICLES
Published on Web 10/19/2002

Very Large Breathing Effect in the First Nanoporous Chromium(III)-Based Solids: MIL-53 or $Cr^{III}(OH)\cdot\{O_2C-C_6H_4-CO_2\}\cdot\{HO_2C-C_6H_4-CO_2H\}_x\cdot H_2O_y$

Christian Serre,*,† Franck Millange,† Christelle Thouvenot,† Marc Noguès,† Gérard Marsolier,‡ Daniel Louër,‡ and Gérard Férey*,†

Contribution from the Institut Lavoisier-Franklin, UFR 2483, Université de Versailles St-Quentin-en-Yvelines, 45 Avenue des Etats-Unis, 78035 Versailles Cedex, France, and Laboratoire de Chimie du Solide et Inorganique Moléculaire, UMR CNRS 6511, Université Rennes I, Avenue du Général Leclerc, 35042 Rennes Cedex, France

Received July 15, 2002

Abstract: The first three-dimensional chromium(III) dicarboxylate, MIL-53as or $Cr^{III}(OH)\cdot\{O_2C-C_6H_4-CO_2\}\cdot\{HO_2C-C_6H_4-CO_2H\}_{0.75}$, has been obtained under hydrothermal conditions (as: as-synthesized). The free acid can be removed by calcination giving the resulting solid, MIL-53ht or $Cr^{III}(OH)\cdot\{O_2C-C_6H_4-CO_2\}$. At room temperature, MIL-53ht adsorbs atmospheric water immediately to give $Cr^{III}(OH)\cdot\{O_2C-C_6H_4-CO_2\}\cdot H_2O$ or MIL-53lt (lt: low-temperature form, ht: high-temperature form). Both structures, which have been determined by using X-ray powder diffraction data, are built up from chains of chromium(III) octahedra linked through terephthalate dianions. This creates a three-dimensional structure with an array of one-dimensional large pore channels filled with free disordered terephthalic molecules (MIL-53as) or water molecules (MIL-53lt); when the free molecules are removed, this leads to a nanoporous solid (MIL-53ht) with a Langmuir surface area over 1500 m^2/g. The transition between the hydrated form (MIL-53lt) and the anhydrous solid (MIL-53ht) is fully reversible and followed by a very high breathing effect (more than 5 Å), the pores being clipped in the presence of water molecules (MIL-53lt) and reopened when the channels are empty (MIL-53ht). The thermal behavior of the two solids has been investigated using TGA and X-ray thermodiffractometry. The sorption properties of MIL-53lt have also been studied using several organic solvents. Finally, magnetism measurements performed on MIL-53as and MIL-53lt revealed that these two phases are antiferromagnetic with Néel temperatures T_N of 65 and 55 K, respectively. Crystal data for MIL-53as is as follows: orthorhombic space group *Pnam* with $a = 17.340(1)$ Å, $b = 12.178(1)$ Å, $c = 6.822(1)$ Å, and $Z = 4$. Crystal data for MIL-53ht is as follows: orthorhombic space group *Imcm* with $a = 16.733(1)$ Å, $b = 13.038(1)$ Å, $c = 6.812(1)$ Å, and $Z = 4$. Crystal data for MIL-53lt is as follows: monoclinic space group *C*2/*c* with $a = 19.685(4)$ Å, $b = 7.849(1)$ Å, $c = 6.782(1)$ Å, $\beta = 104.90(1)°$, and $Z = 4$.

Introduction

The synthesis of hybrid inorganic−organic nanoporous solids is still a matter of high concern since this approach gives a new dimension to the domain of porous compounds.[1−5] The large number of existing organic linkers and the unique physical properties of inorganic materials lead to a modulation of both the shape of the pores and the properties of the final porous materials. In these structures, organic moieties, such as diphosphonates or dicarboxylates, act as pillars or linkers relating inorganic layers, chains, or clusters of transition or rare-earth metals.

In the field of metal carboxylates synthesized under hydrothermal conditions, there is an increasing number of three-dimensional porous or pillared solids reported to date such as zinc,[6] nickel,[7] and cobalt.[8−10] Under soft solvothermal conditions, Yaghi and coworkers recently used the secondary building units approach to synthesize nanoporous hybrid solids with a modulate pore size.[11] However, these solids are coordination polymers built up from clusters of divalent cations (Zn, Cu, ...) related by dicarboxylate anions. To date, both approaches (hydro or solvothermal) have not really been extended to higher oxidation state elements, and porous hybrid solids based on tri- or tetravalent cations are very scarce. Recently, our group reported a few porous vanadium(III or IV) dicarboxylates.[12,13]

* Address correspondence to either author. E-mail: (C.S.) serre@chimie.uvsq.fr and (G.F.) ferey@chimie.uvsq.fr.
† Université de Versailles St-Quentin-en-Yvelines.
‡ Université Rennes I.

(1) Férey, G. *J. Solid State Chem.* **2000**, *152*, 37.
(2) O'Keeffe, M.; Eddaoudi, M.; Li, H.; Reineke, T.; Yaghi, O. M. *J. Solid State Chem.* **2000**, *152*, 3.
(3) Feng, S.; Xu, R. *Acc. Chem. Res* **2001**, *34*, 239.
(4) Férey, G. *Chem. Mater.* **2001**, *13*, 3084.
(5) Clearfield, A. *Curr. Opin. Solid State Mater. Sci.* **1996**, *1*, 268.
(6) Ogata, S.; Tagaya, H.; Kadokawa, J. *J. Mater. Chem.* **2000**, *10*, 321.
(7) Forster, P. M.; Cheetham, A. K. *Angew. Chem., Int. Ed.* **2002**, *41*, 457.
(8) Livage, C.; Guillou, N.; Marrot, J.; Férey, G. *Chem. Mater.* **2001**, *13*, 4387.
(9) Huang, Z.-L.; Drillon, M.; Masciocchi, N.; Sironi, A.; Zhao, J.-T.; Rabu, P.; Panissod, P. *Chem. Mater.* **2000**, *12*, 2805.
(10) Kumagai, H.; Kepert, C. J.; Kurmoo, M. *Inorg. Chem.* **2002**, *41*, 3410.
(11) Eddaoudi, M.; Moler, D. B.; Li, H.; Chen, B.; Reineke, T.; O'Keefe, M.; Yaghi, O. M. *Acc. Chem. Res* **2001**, *34*, 319.

In the field of chromium-based porous solids, results are very scarce mainly because of the chemical inertness of chromium.[14,15] Only a few porous solids incorporating chromium have been characterized to date.[16] Chromium incorporating cyano-bridged transition metal solids have also been described recently by Verdaguer in an attempt to establish high-temperature ferromagnets, but these solids are coordination polymers with no porosity.[17]

We recently initiated a global study of the chromium dicarboxylate system in water, and we report here our first results (i.e., the synthesis and characterization of the first three-dimensional chromium(III) dicarboxylates: MIL-53as or $Cr^{III}(OH)\cdot\{O_2C-C_6H_4-CO_2\}\cdot\{HO_2C-C_6H_4-CO_2H\}_{0.75}$, MIL-53ht or $Cr^{III}(OH)\cdot\{O_2C-C_6H_4-CO_2\}$, and MIL-53lt or $Cr^{III}(OH)\cdot\{O_2C-C_6H_4-CO_2\}\cdot H_2O$).[18]

Experimental Section

Synthesis. MIL-53as was hydrothermally synthesized (autogenous pressure) from a mixture of chromium(III) nitrate $Cr(NO_3)_3\cdot 9H_2O$ (Aldrich, 97%), terephthalic acid $HO_2C-(C_6H_4)-CO_2H$ (Alfa 97%), hydrofluoric acid (HF) (Prolabo, 40%), and H_2O in the molar ratio 1:1:1:280. Reactants were introduced in this order and stirred a few minutes before introducing the resulting suspension in a Teflon-lined steel autoclave, and the temperature was set at 493 K for 3 days. The pH remained very acidic (<1) during the course of the synthesis. A light purple powder was finally obtained together with traces of terephthalic acid. All the attempts for getting crystals of MIL-53as failed. The calcined form MIL-53ht was obtained by calcination of MIL-53as at 300 °C under air atmosphere; it adsorbs water at room temperature to give MIL-53lt or $Cr^{III}(OH)\cdot\{O_2C-C_6H_4-CO_2\}\cdot H_2O$.

Elementary Analysis. Quantitative elemental analyses indicating C/Cr and H/Cr ratios, respectively, were equal to 13.5:7.7 and 9.1:6.1 for MIL-53as and MIL-53lt, which are in good agreement with the theoretical values of 14:8 and 9:6. The slightly lower observed C/Cr ratios are due to the presence of a small amount of poorly crystallized Cr_2O_3 in both cases.

Thermogravimetry. TGA experiments, performed under air atmosphere (5 °C/min) on MIL-53as and MIL-53lt using a TA Instrument type 2050 analyzer apparatus, have shown several weight losses in the 353−873 K range. The residual solid has been identified as poorly crystallized chromium oxide Cr_2O_3. MIL-53as exhibits two weight losses, not well separated, of 28 and 50% at approximately 723 and 773 K, corresponding respectively to the departures of the free and the bound terephthalic acid, followed by their partial replacement by oxygen atoms to form chromium oxide at higher temperatures (see Thermal Behavior section). These losses are on the whole in agreement with the theoretical values (total loss: 78.7%). MIL-53lt exhibits a similar weight loss of 60% at 723 K and also a 7.3% loss at 353 K, corresponding to the departure of the diacid and free water molecules (theoretical: 62 and 7.2%).

Infrared Spectroscopy. The infrared spectra of the title compounds clearly show the presence of the vibrational bands characteristic of the framework −(O−C−O)− groups around 1550 and 1430 cm^{-1} confirming the presence of the dicarboxylate within the solid; a band at 1700 cm^{-1} characteristic of free −C═O groups is also observed for MIL-53as but not for MIL-53lt, which is in agreement with the absence of free acid within the pores for this solid. Bands around 3500 cm^{-1} also confirmed the presence of OH and/or H_2O groups for both phases.

Temperature-Dependent X-ray Diffraction. X-ray thermodiffractometry, performed in the furnace of a Siemens D-5000 diffractometer in the $\theta-\theta$ mode under air, shows several steps in the decomposition of MIL-53as (see Thermal Behavior section) and the reversible dehydration of MIL-53lt. Each pattern was recorded within the 7−35° range (2θ) with a 2 s/step scan, which gave an approximate 1 h length for each pattern at the corresponding temperature. The heating rate between two temperatures was 5 °C/min.

Sorption Experiments. Acetone (SDS, 99.5%), ethanol (Prolabo, 99%), and dimethylformamide (DMF) (SDS, 99%) were used without any purification during the study of sorption properties of MIL-53lt.

Magnetic Measurements. Experiments were performed on both powder samples MIL-53as and MIL-53lt over the temperature range of 5−300K, with a SQUID magnetometer for an external applied magnetic field B of 0.5 T. The samples have been first zero-field cooled, and the magnetic field was applied after stabilization of the temperature at 4.5 K.

Results and Discussion

Structure Solution. All attempts for getting single crystals of MIL-53as failed. The powder X-ray diffraction patterns of MIL-53as and MIL-53lt were collected on a D5000 ($\theta-2\theta$ mode) Siemens diffractometer with λ (Cu $K\alpha_1$, $K\alpha_2$) = 1.54059, 1.54439 Å. In the case of MIL-53ht, a temperature in situ data collection was performed at 523 K using a D5000 ($\theta-2\theta$ mode) Siemens diffractometer equipped with an Anton Paar HTK1200 oven.

The cell parameters of the vanadium analogue, MIL-47as and MIL-47,[12] were thus used as the starting point of the structure determination for MIL-53as and MIL-53ht. However, space groups of MIL-53ht and MIL-53as were different (*Imcm* instead of *Pnam*). Attempts of indexation of the pattern of MIL-53lt were unsuccessful because of an anisotropic enlargement of some reflections; however, during the course of this study, the aluminum isostructural solid MIL-53(Al)lt was synthesized in our group with surprisingly no peak enlargement,[19] and its structure was solved using Expo.[20] Then, its final atomic positions were used to solve the structure of MIL-53lt. Thus, after a pattern matching was performed with Fullprof2k using the WinPLOTR software package,[21,22] refinements of MIL-53as and MIL-53lt used atomic coordinates of MIL-47as and MIL-53(Al)lt, respectively, whereas a direct method (using Expo) was achieved to solve the structure of MIL-53ht. All the structures were refined using Fullprof2k. A small impurity was present and refined as a secondary phase: terephthalic acid and chromium oxide Cr_2O_3 for MIL-53as and MIL-53lt, ht, respectively. Full details of the structure determination are reported in the Supporting Information. Bond valence calculation leads to the values of 3.1, 3.3, and 3.0 for the valence of chromium atoms for MIL-53as, MIL-53ht, and MIL-53lt, respectively.[23]

The formulas deduced from the structure determination for MIL-53as, MIL-53ht, and MIL-53lt are as follows: $Cr^{III}(OH)\cdot$

(12) Barthelet, K.; Marrot, J.; Riou, D.; Férey, G. *Angew. Chem., Int. Ed.* **2002**, *41*, 281.
(13) Barthelet, K.; Riou, D.; Férey, G. *Chem. Commun.* **2002**, 1492.
(14) Baes, C.; Mesmer, R. E. *The Hydrolysis of Cations*; Krieger Publishing Company: Malabar, FL, 1986.
(15) Jolivet, J. P. *De la Solution a L'oxyde*; CNRS Editions: Paris, 1994.
(16) Kornatowski, J.; Zadrozna, G.; Rozwadowski, M.; Zibrowius, B.; Marlow, F.; Lercher, J. A. *Chem. Mater.* **2001**, *13*, 4447.
(17) Verdaguer, M. *Science* **1996**, *272*, 696.
(18) Millange, F.; Serre, C.; Férey, G. *Chem. Commun.* **2002**, 822.
(19) Loiseau, T. Manuscript in preparation.
(20) Altomare, A.; Burla, M. C.; Camalli, M.; Carrozzini, B.; Cascarano, G. L.; Giacovazzo, C.; Guagliardi, A.; Moliterni, A. G. G.; Polidori, G.; Rizzi, R. *J. Appl. Crystallogr.* **1999**, *32*, 339.
(21) Rodriguez-Carvajal, J. *Collected Abstracts of Powder Diffraction Meeting*, Toulouse, France, 1990; p 127.
(22) Roisnel, T.; Rodriguez-Carvajal, J. *Abstracts of the 7th European Powder Diffraction Conference*, Barcelona, Spain, 2000; p 71.
(23) Brese, N. E.; O'Keeffe, M. *Acta Crystallogr.* **1991**, *B47*, 192.

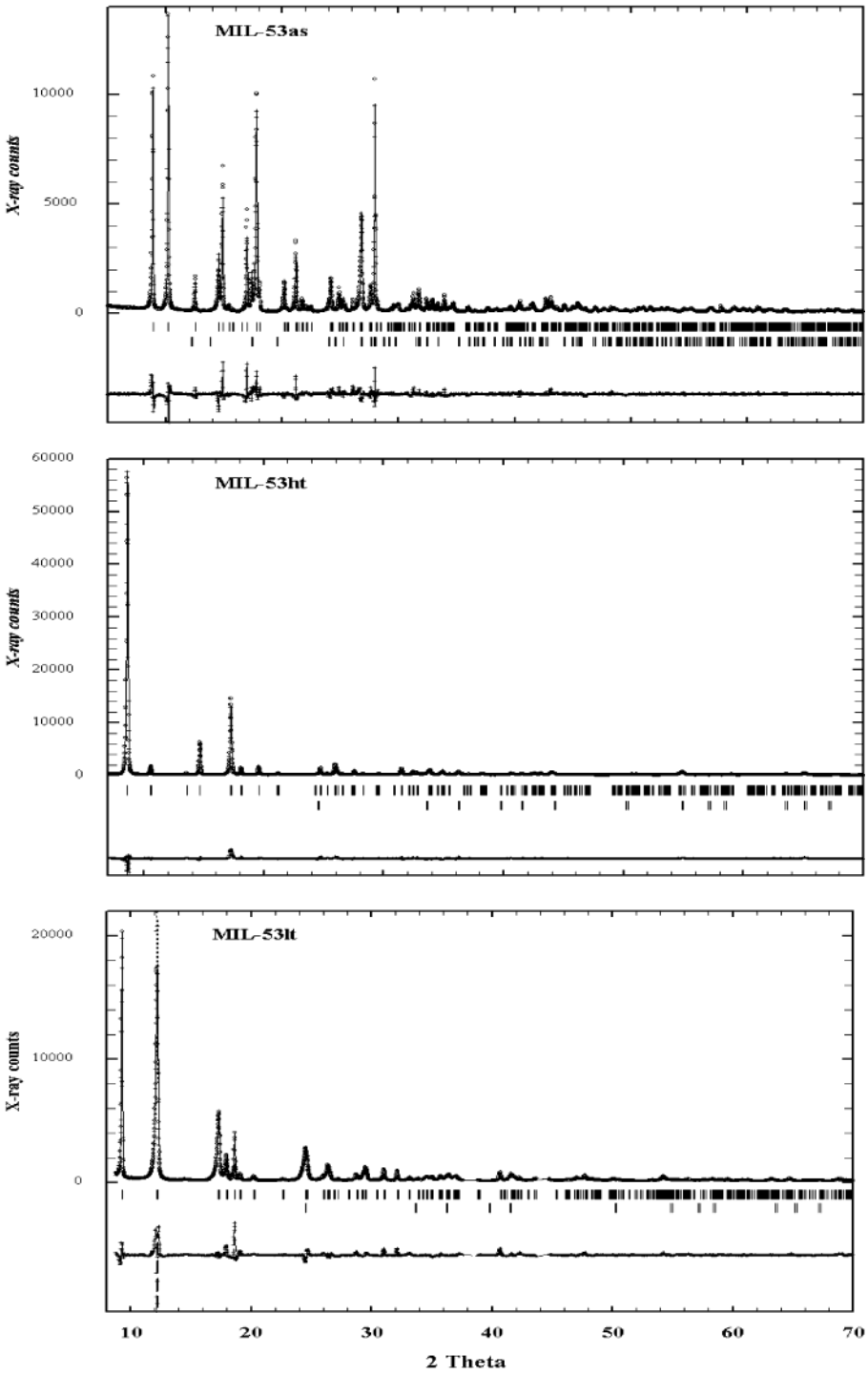

Figure 1. Final Rietveld plot of (a) MIL-53as, (b) MIL-53ht, and (c) MIL-53lt.

Table 1. Crystal Data for MIL-53as, MIL-53ht, and MIL-53lt or $Cr^{III}(OH)\cdot\{O_2C-C_6H_4-CO_2\}\cdot\{HO_2C-C_6H_4-CO_2H\}_{0.75}$, $Cr^{III}(OH)\cdot\{O_2C-C_6H_4-CO_2\}$, and $Cr^{III}(OH)\cdot\{O_2C-C_6H_4-CO_2\}\cdot H_2O$

formula	MIL-53as	MIL-53ht	MIL-53lt
crystal system	orthorhombic	orthorhombic	monoclinic
space group	*Pnam* (No. 62)	*Imcm* (No. 74)	*C*2/*c* (No. 15)
a (Å)	17.340(1)	16.733(1)	19.685(4)
b (Å)	12.178(1)	13.038(1)	7.849(1)
c (Å)	6.822(1)	6.812(1)	6.782(1)
β (°)			104.90(2)
no. of reflections	355	271	211
R_P	11.9	10.0	14.5
R_{WP}	15.8	13.2	19.4
R_B	6.6	7.9	8.5

$\{O_2C-C_6H_4-CO_2\}\cdot\{HO_2C-C_6H_4-CO_2H\}_{0.75}$, $Cr^{III}(OH)\cdot\{O_2C-C_6H_4-CO_2\}$, and $Cr^{III}(OH)\cdot\{O_2C-C_6H_4-CO_2\}\cdot H_2O$. The final agreement factors[24] (see Table 1) are satisfactory for MIL-53as and MIL-53ht, while values are slightly higher for MIL-53lt because of the anisotropic enlargement. The origin of the peak enlargement will be discussed further in the paper. The corresponding Rietveld plots are reported in Figure 1. Atomic coordinates are given in Table 2.

Structure Description. MIL-53as, MIL-53ht, and MIL-53lt exhibit a three-dimensional structure built up from chromium-

(24) Young, R. A.; Wiles, D. B. *J. Appl. Crystallogr.* **1982**, *15*, 430.

Table 2. Atomic Coordinates

atom	x/a	y/b	z/c
		MIL-53as	
Cr	0	0	0
O(1)	0.002(2)	−0.078(1)	−0.250
O(2)	0.089(1)	0.089(1)	−0.087(2)
O(3)	0.073(1)	−0.112(1)	0.090(2)
C(1)	0.108(2)	−0.143(3)	0.250
C(2)	0.123(2)	0.117(4)	−0.250
C(3)	0.171(2)	−0.213(3)	0.250
C(4)	0.191(2)	0.180(4)	−0.250
C(5)	0.229(1)	0.198(2)	−0.078(2)
C(6)	0.205(1)	−0.236(2)	0.080(2)
X(7a)[a]	0.032(2)	0.309(3)	−0.250
X(8a)	0.133(4)	−0.465(4)	−0.051(2)
X(9a)	0.144(3)	0.451(3)	−0.250
X(10a)	0.138(2)	0.473(2)	0.134(3)
X(11a)	−0.034(2)	−0.350(3)	−0.250
X(12a)	0.032(2)	0.369(2)	0.043(4)
X(13a)	0.101(1)	0.405(2)	−0.013(6)
X(14a)	0.046(3)	0.425(3)	−0.190(1)
		MIL-53ht	
Cr	0.250	−0.250	0.250
O(1)	0.250	0.686(1)	0
O(2)	0.166(1)	0.843(1)	0.156(1)
C(1)	0.040(1)	0.982(1)	−0.196(1)
C(2)	0.054(1)	0.961(2)	0
C(3)	0.125(1)	0.888(2)	0
		MIL-53lt	
Cr	0	0	0
O(1)	0	−0.113(1)	−0.250
O(2)	0.068(1)	0.166(1)	0.945(1)
O(3)	0.087(1)	0.141(1)	0.652(1)
O(4)	0	0.500	0.500
C(1)	0.111(1)	0.190(1)	0.830(1)
C(2)	0.198(1)	−0.296(2)	0.618(1)
C(3)	0.271(1)	−0.320(2)	0.704(1)
C(4)	0.184(1)	−0.210(2)	0.421(1)

[a] With X = C or O.

(III) octahedra and terephthalate ions, creating a three-dimensional framework with a one-dimensional pore channel system (Figure 2). As reported before,[18] pores of MIL-53as or $Cr^{III}(OH)\cdot\{O_2C-C_6H_4-CO_2\}\cdot\{HO_2C-C_6H_4-CO_2H\}_{0.75}$ are filled with disordered free terephthalic acid that can be removed by calcination to give MIL-53ht or $Cr^{III}(OH)\cdot\{O_2C-C_6H_4-CO_2\}$. This latter hydrates at room temperature to give MIL-53lt or $Cr^{III}(OH)\cdot\{O_2C-C_6H_4-CO_2\}\cdot H_2O$; the water molecules are located at the center of the pores, strongly interacting through hydrogen bonds with oxygen atoms or hydroxyl groups of the inorganic network.

In both structures, corner-sharing chromium octahedra are linked through μ_2(OH) bridging groups. Bond valence calculations give a valence of approximately 1.07, 1.25, and 1.01 for these oxygen atoms, which is in agreement with infrared spectrum results, whereas a narrow band at 3500 cm^{-1} suggests the presence of −OH groups. The chains are then related together with dicarboxylates creating the three-dimensional nanoporous structure (Figures 2 and 3). The anions of chromium octahedra are two OH groups in trans position and four oxygen atoms coming from the dicarboxylates.

The interatomic distances are, in both cases, close to those usually reported for chromium(III) solids: Cr−O distances are between 1.90 and 2.08 Å. C−O and C−C distances are also usual, within the ranges of 1.24−1.39 and 1.33−1.53 Å, respectively.

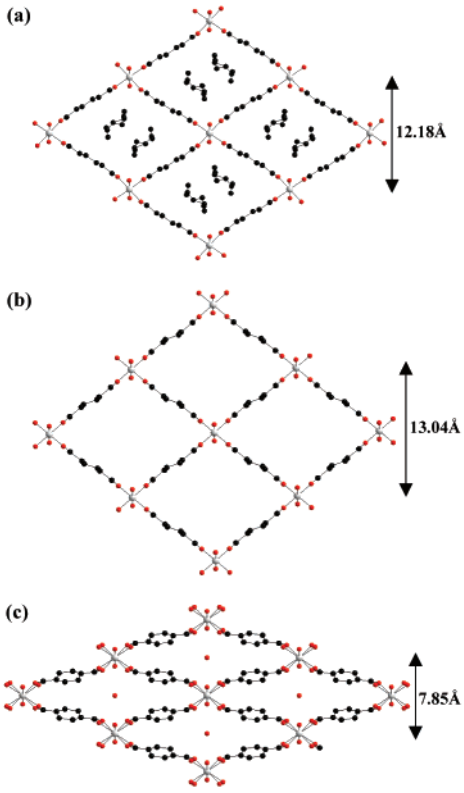

Figure 2. View of the pore systems of (a) MIL-53as, (b) MIL-53ht, and (c) MIL-53lt.

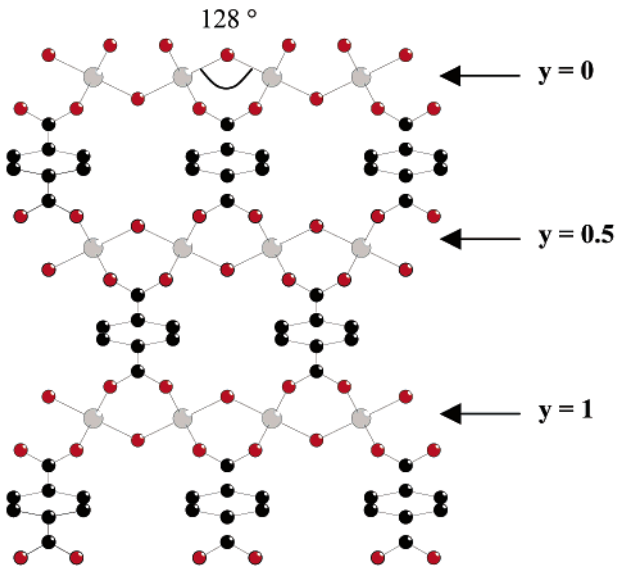

Figure 3. View perpendicular to the pores of MIL-53ht.

Unlike in the case of the isostructural vanadium phase MIL-47as, reported recently by Barthelet et al.,[12] calcination of the as-synthesized chromium solid is not followed by an oxidation of the cation. Both chromium compounds contain only chromium(III) instead of vanadium(III) and vanadium(IV) for MIL-47as and MIL-47, respectively.

The presence of water molecules in MIL-53lt was unexpected since no water is present in MIL-47 because of the hydrophobic character of the pore walls built mainly from aromatic rings. However, unlike in the case of MIL-47 where the bridging groups of the vanadyl chains are oxygen atoms, the presence

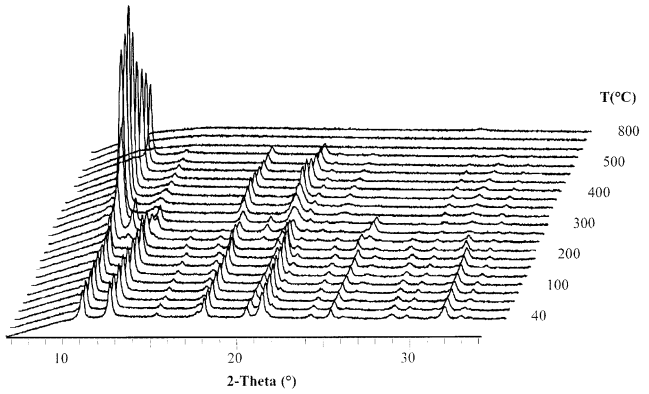

Figure 4. X-ray thermodiffractogram of MIL-53as under air; for a better understanding, a 2θ offset is applied for each pattern.

of hydroxyl groups within the inorganic chains of MIL-53lt stabilizes a water molecule, one H_2O per OH, through hydrogen bonding interactions.

Structures of MIL-53as, MIL-53ht, and MIL-53lt are very similar despite the absence of free organic molecules in the two latter solids; however, the cell parameters, characteristic of the pores, change significantly upon calcination and/or hydration. This will be discussed in the next section.

Thermal Behavior. A first X-ray thermodiffractometry experiment was performed under air atmosphere between room temperature and 800 °C (1073 K) for MIL-53as. As shown in Figure 4, MIL-53as is stable up to 375 °C, and three major structural changes occur respectively at 250, 300, and 400 °C (see following scheme).

$$\mathrm{Cr(OH)\cdot\{O_2C-C_6H_4-CO_2\}\cdot\{HO_2C-C_6H_4-CO_2H\}_{0.75}} \xrightarrow{T > 250\ ^\circ\mathrm{C}} \mathrm{Cr(OH)\cdot\{O_2C-C_6H_4-CO_2\}\cdot\{HO_2C-C_6H_4-CO_2H\}_{0.5}}$$

$$\mathrm{Cr(OH)\cdot\{O_2C-C_6H_4-CO_2\}\cdot\{HO_2C-C_6H_4-CO_2H\}_{0.5}} \xrightarrow{T > 300\ ^\circ\mathrm{C}} \mathrm{Cr(OH)\cdot\{O_2C-C_6H_4-CO_2\}}$$

$$\mathrm{Cr(OH)\cdot\{O_2C-C_6H_4-CO_2\}} \xrightarrow[\cdot\{O_2C-C_6H_4-CO_2\} + 0.5O_2]{T > 400\ ^\circ\mathrm{C},} \text{amorphous } \mathrm{Cr_2O_3}$$

The first two changes are in agreement with TGA results (Figure 5) and are attributed to the two-step departure of the free disordered acid (T > 250 °C), and the last one is attributed to the departure of the framework diacid. The first loss leads to the crystallization of an intermediate phase. This latter was isolated by calcination of MIL-53as overnight at 275 °C, and analysis gave an approximate composition of $Cr^{III}(OH)\cdot\{O_2C-C_6H_4-CO_2\}\cdot\{HO_2C-C_6H_4-CO_2H\}_{0.5}$ for this solid. At 300 °C, this phase disappears to the benefit of MIL-53ht or $Cr^{III}(OH)\cdot\{O_2C-C_6H_4-CO_2\}$, which exhibits a type I adsorption−desorption isotherm and a very high Langmuir surface area (>1500 m^2/g).[18] At higher temperatures, the departure of the framework diacid leads to an amorphous solid. One can point out the differences in thermal behavior between TGA and thermodiffractometry results. This comes from the difference in heating processes; both experiments use the same heating rate, but thermodiffractometry uses steps corresponding to the acquisition of the patterns.

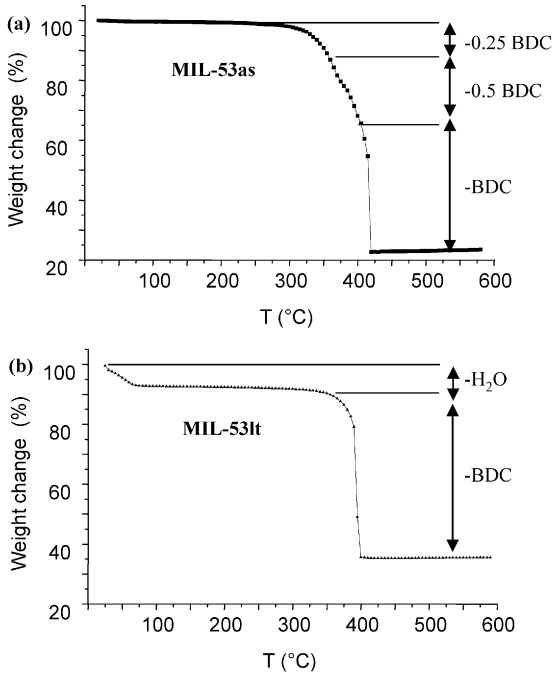

Figure 5. TGA under air of MIL-53as and MIL-53lt.

Study of the Breathing Effect. As reported before, cell parameters evolve upon calcination and hydration. If the cell parameter characteristic of the chains remains constant in both cases (≈6.8 Å), the *a* and *b* parameters delimiting the pores change significantly for MIL-53as and MIL-53ht from 17.34 to 16.73 Å and from 12.18 to 13.04 Å, respectively. This breathing effect is, however, much more pronounced during the hydration−dehydration process as the parameters change for MIL-53ht and MIL-53lt from 16.73 (*a*) to 19.0 Å (*a* sin θ) and from 13.04 (*b*) to 7.85 Å (*b*), respectively (Figure 6). If the cell volume does not really change during calcination (from 1440 up to 1480 $Å^3$), it strongly decreases upon hydration (1012 $Å^3$), indicating a significant anisotropic contraction of the pores along the *b* axis. As a consequence, both MIL-53as (with the presence of free dicarboxylic acid within the pores) and MIL-53lt (filled with water molecules) do not exhibit any accessible porosity, while MIL-53ht possesses large pores of approximately 8.6 × 8.6 Å or 9.4 × 11.4 Å *free* aperture, taking into account the van der Waals radius of atoms, depending on distances either between carbons of organic rings or between hydroxyl groups of chromium octahedra delimiting the pores.

In a second step, the thermal study of MIL-53lt was performed. In agreement with TGA results (Figure 5), a structural change was expected for this solid, and a second X-ray thermodiffractometry experiment was realized on MIL-53lt by heating and cooling between room temperature and 200 °C (473 K) (Figure 6). It appears clearly that the hydration−dehydration process of MIL-53ht−MIL-53lt is fully reversible, indicating a zeolithic behavior for MIL-53lt. The opening and closing of the pores that occurs upon dehydration and hydration is thus reversible, indicating a very large breathing effect never observed before at such a scale for a nanoporous solid. It involves a displacement of the chains by 5.2 Å during hydration without any change of the topology. This outstanding effect is probably due to two conjugated phenomena: (i) the creation of strong hydrogen bonds between the water molecule and the hydrophilic parts of the pore (i.e., oxygen atoms and OH groups

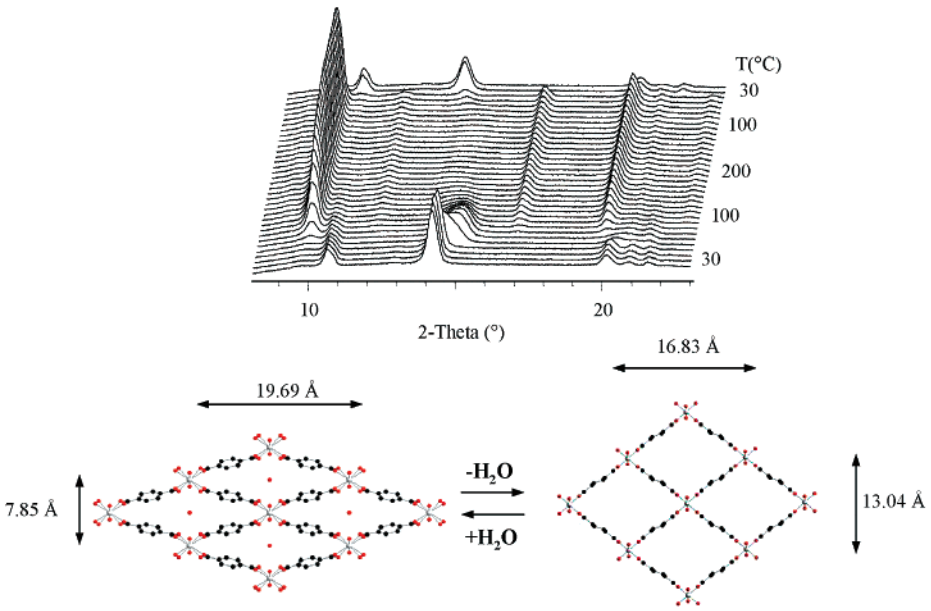

Figure 6. (top) Schematic representation of the reversible hydration−dehydration of MIL-53lt and MIL-53ht. (bottom) X-ray thermodiffractogram of MIL-53lt under air; for a better understanding, a 2θ offset is applied for each pattern.

(d(Ow−O) ≈ 3−3.4 Å)) and (ii) the onset of $\pi-\pi$ interactions because of the benzyl groups (d(C−C) ≈ 3.9−4.5 Å). This large breathing phenomenom is relatively quick (a few minutes) and is followed by an important contraction of the powder; as no reflection broadening was observed for *h*00 reflections on the X-ray pattern, this might lead to the formation of structural defects (stacking faults?) along a direction perpendicular to the *a* axis. This would explain why an anisotropic peak enlargement is observed for MIL-53lt.

Sorption Study. Adsorption of organic solvents was tried with MIL-53lt. First, acetone or ethanol was tested (50 mg of product in 25 mL of solvent). Unlike in the case of MIL-47, X-ray diffraction and TGA both confirmed that no acetone or ethanol could be incorporated in MIL-53lt even after 4 days of immersion in the solvent. In a second step, adsorption of solvents was tried on MIL-53lt by dispersing the dehydrated powder (heated at 200 °C) directly into acetone or ethanol. Again, no solvent could be incorporated since MIL-53ht adsorbed some traces of water present in the solvents to form again MIL-53lt. In a last step, adsorption of DMF was tried directly on MIL-53lt using the same process. Unlike in the case of acetone or ethanol, DMF was incorporated into the pores, giving the solid MIL-53solv or $Cr^{III}(OH)\cdot\{O_2C-C_6H_4-CO_2\}\cdot$DMF. In Figure 7a, the X-ray pattern of this latter solid at room temperature shows some similarities with those of MIL-53as. TGA of MIL-53solv showed two weight losses of 20 and 52%, which is on the whole in agreement with the departure of one DMF/Cr (calcd: 23.6%) and the dicarboxylic acid (calcd: 48.5%) (Figure 7b). Infrared spectroscopy indicates the presence of the free −C═O bands of the DMF moieties at 1700 cm^{-1} (Figure 7c). These results confirm the incorporation of the DMF molecules within the pores. Thus, replacement of water molecules by DMF moieties into MIL-53lt indicates that cages of MIL-53 show a better affinity for DMF molecules than for water. This comes probably from the higher capability of DMF toward the formation of strong hydrogen bonds with the hydroxyl groups of the inorganic chains; in fact, DMF is able to form by delocalization of π electrons (resonance) $-N^+=C-O^-$ groups

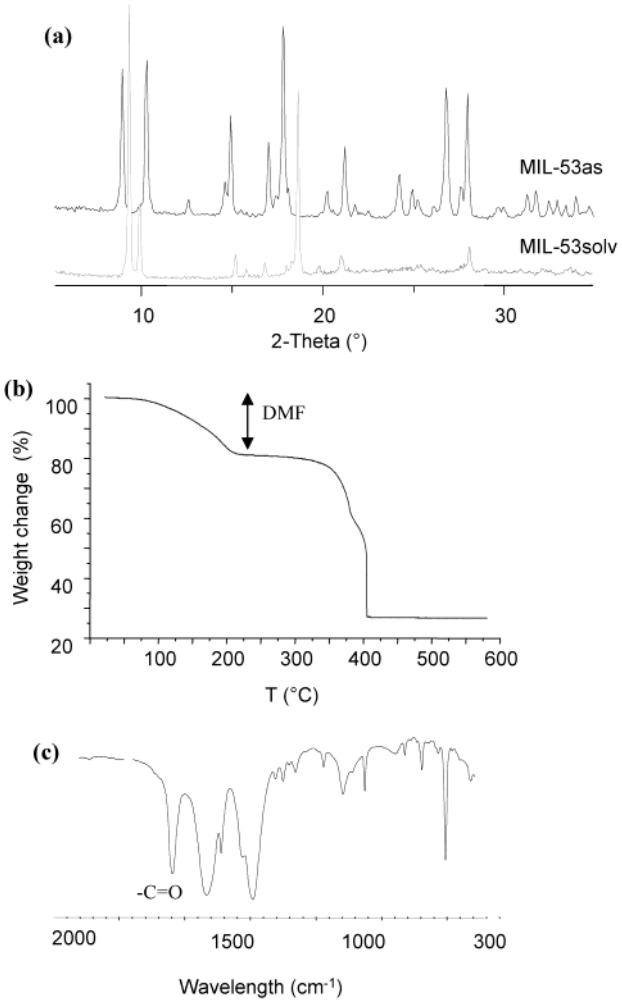

Figure 7. (a) Comparison of the X-ray patterns of MIL-53solv and MIL-53as, (b) TGA under air of MIL-53solv (solv = DMF), and (c) infrared spectrum of MIL-53solv.

that are better candidates than H_2O molecules for realizing hydrogen bonds. It seems surprising that a polar solvent such

Table 3. Cell Parameters for MIL-53 Inserting Different Moieties

solid	*a* (Å)	*b* (Å)	*c* (Å)	*β* (deg)	*V* (Å^3)	adsorbed molecule
MIL-53lt	19.685(4)	7.849(1)	6.782(1)	104.90(2)	1012.8(1)	H_2O
MIL-53solv	17.905(1)	11.218(1)	6.825(1)		1370.7(1)	DMF
MIL-53as	17.340(1)	12.178(1)	6.822(1)		1440.6(1)	1,4-BDC

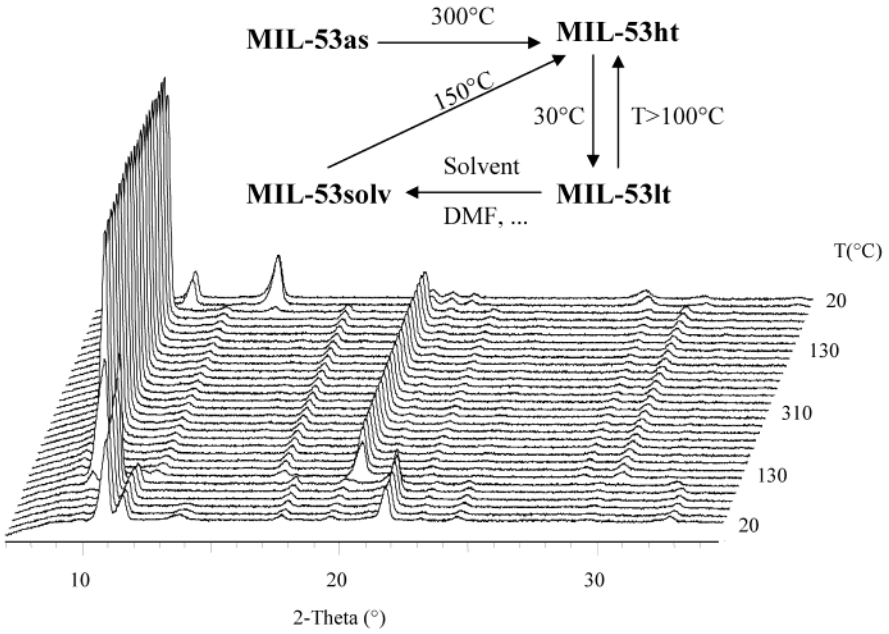

Figure 8. X-ray thermodiffractogram of MIL-53solv under air; for a better understanding, a 2θ offset is applied for each pattern. A schematic representation of the hydration−dehydration and sorption of solvent of MIL-53 is included at the top of the figure.

as ethanol cannot get into the pores of MIL-53; this might be due to the higher affinity of MIL-53 for water (present as traces in ethanol) as compared with ethanol. This comes probably from the higher capability of water for establishing hydrogen bonds. Further sorption studies using other organic solvents are currently in progress.

The X-ray pattern of MIL-53solv has been indexed with satisfactory figures of merit giving the following cell parameters: $a = 17.905(1)$ Å, $b = 11.218(1)$ Å, $c = 6.825(1)$ Å, $Z = 4$, $V = 1370.7(1)$ Å^3, and space group *Pnam*. One observes that the cell parameters of the MIL-53solv are intermediate between the cell parameters of MIL-53as and MIL-53lt (see Table 3)**.** Therefore, the cell volume and indirectly the size of the cage increase with the size of the molecule inserted in the pores: H_2O < DMF < terephthalic acid. This shows again the very high breathing ability of these solids.

Finally, a third X-ray thermodiffractometry experiment was realized on MIL-53solv heating and cooling between room temperature and 300 °C (573 K) (Figure 8). It appears that DMF molecules leave the pores upon heating without any destabilization of the framework to form at high-temperature MIL-53ht and again MIL-53lt when cooling back to room temperature. The whole process is summarized as an insert of Figure 8.

Magnetic Properties. The inverse molar susceptibility curves $1/\chi_{dc}$ revealed an antiferromagnetic behavior with Néel temperature T_N of 65 K for MIL-53as and a canted antiferromagnetic behavior with T_N of 55 K for MIL-53lt (Figure 9). This could be explained by the difference of the Cr−O−Cr angle between the two structures (121.5 and 124.8°, respectively). The

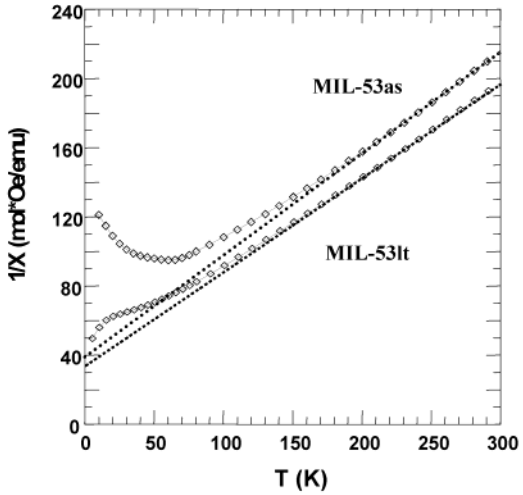

Figure 9. Susceptibility measurement vs temperature of MIL-53as and MIL-53lt.

fit of the linear part of $1/\chi_{dc}$, established after correction of the sample holder signal and the core diamagnetism, follows a Curie−Weiss law $\kappa_{dc} = C/(T - \theta_p)$. This leads to a negative paramagnetic Curie temperature (of approximately $\theta_p = -75$ K in both cases), indicative of antiferromagnetic interactions. For Cr^{3+}, the orbital momentum is quenched so that S is the appropriate quantum number: $\mu_{eff} = g[S(S + 1)]^{1/2}\,\mu_B$, with $g = 2$ and $S = 3/2$, which leads to $\mu_{eff} = 3.87\,\mu_B$ for Cr^{3+}. The Curie constant deduced from the linear part of the $1/\chi_{dc}$ curves gives an effective moment $\mu_{eff} = 3.69$ and $3.79\,\mu_B$ for MIL-53as and MIL-53lt, close to the theoretical value.

Conclusion

Finally, MIL-53 solids (as, lt, ht) are the first nanoporous chromium-based solids reported to date. These solids exhibit original properties such as zeolithic behavior associated with a very large breathing effect, magnetic properties, a high thermal stability, and sorption capacities. The use of chromium opens now the way for the synthesis and characterization of new porous solids with potential applications. Other results are in progress and will be published soon.

Acknowledgment. The authors gratefully acknowledge Dr. T. Loiseau for his collaboration in determining the structure of MIL-53lt.

Supporting Information Available: Full details of the structure determination as well as bond distances tables. Infrared spectra of solids MIL-53as and MIL-53lt and the N_2 adsorption−desorption isotherm. This material is available free of charge via the Internet at http://pubs.acs.org.

JA0276974